References and Notes

1. A. Pannekoek, *Astron. Nachr.* **164**, No. 3913 (1903); C. Fabry, *J. Obs.* **12**, 1 (1929); D. W. Goldsmith, *Icarus* **2**, 341 (1963); R. Brinkmann, *Nature* **230**, 515 (1971).
2. G. E. Taylor, B. O'Leary, T. C. Van Flandern, P. Bartholdi, F. Owen, W. B. Hubbard, B. A. Smith, S. A. Smith, F. W. Fallon, E. J. Devinney, J. Oliver, *Nature* **234**, 405 (1971).
3. W. A. Baum and A. D. Code, *Astron. J.* **58**, 108 (1953).
4. D. H. Menzel and G. de Vaucouleurs, *Final Report on the Occultation of Regulus by Venus, July 7, 1959* [ARDC contract AF 19 (604)-7461, Air Force Research and Development Command, Bedford, Mass., 1961]; G. E. Taylor, *Roy. Observ. Bull.* **72**, E355 (1963).
5. G. E. Taylor, *Nature* **219**, 474 (1968); *Mon. Notic. Roy. Astron. Soc.* **147**, 27 (1970); G. Lynga, K. C. Freeman, M. J. Miller, K. Serkowski, N. Stokes, *Proc. Astron. Soc. Aust.* **1**, 201 (1969); K. C. Freeman and G. Lynga, *ibid.*, p. 203; *Astrophys. J.* **160**, 767 (1970).
6. J. Meeus, *J. Br. Astron. Assoc.* **70**, 174 (1960); P. Ahnert and J. Meuss, *ibid.* **71**, 123 (1961).
7. C. W. Allen, *Astrophysical Quantities* (Athlone, London, ed. 2, 1963), pp. 201, 234–36.
8. The American Ephemeris and Nautical Almanac is published annually by the Nautical Almanac Office, U.S. Naval Observatory, Washington, D.C.
9. I. Halladay, R. H. Hardie, O. Franz, J. B. Priser, *Astron. J.* **70**, 676 (1965).
10. These predictions are published in the handbook of the British Astronomical Association, and a copy is sent to the Royal Astronomical Society of Canada. Important events are also announced in circulars put out by the International Astronomical Union. An outline of predictions for the next 9 years was written by G. E. Taylor for presentation at the meeting of the American Astronomical Society, Division for Planetary Sciences, in Tallahassee, Florida, February 1971, and is available upon request from the Royal Greenwich Observatory, Greenwich, England. T. Van Flandern of the U.S. Naval Observatory has advised me that the AGK 3 star catalog [*Astronomische Gesellschaft Katalog* (Engelmann, Bonn, Germany), vol. 3] is also on magnetic tape and could be used to predict occultations of stars north of −2° declination, down to magnitude 10.5. Such a program would be useful as a check to the existing program based on the star catalog of the Smithsonian Astrophysical Observatory and would allow a much larger popuation of stars to be applied to prediction of occultations by the Galilean satellites, Titan, Neptune, and the asteroids.
11. This work is being carried out by G. E. Taylor upon special request by individual scientists.
12. Studies are under way to find methods of sharpening predictions once the initial announcement is made. For example, star positions can be remeasured on plates, and residuals from the ephemerides for the planet or satellite, or both, can be studied. With 2 weeks notice, it was possible to improve the accuracy of observation of the occultation of Beta Scorpii C by Io to about 0.2 arc second in the direction perpendicular to the motion of the satellite.
13. I quote a reviewer of this paper about the need for cooperation: "If predictions are to be extended in some cases to objects as faint as magnitude 17 or 18, this cooperation will have to extend to those astronomers with suitable astrometric instruments and skills. It is certainly true that predictions in the past have been hampered by inadequate astrometry, coupled with the use of ephemerides that are not as good as they should be (e.g. the Pluto miss in March 1971). Satisfactory ephemerides for all the major and large minor planets can and should be supplied; the satellites are more of a problem, but given time this can be solved too (and fortunately, as the author points out, in some cases one has the advantage of size)."
14. I thank Drs. T. Van Flandern, G. E. Taylor, and R. Brinkmann for helpful discussions and correspondences.

* Presently at the Department of Interdisciplinary Sciences, San Francisco State College, California, and National Aeronautics and Space Administration, Ames Research Center, Moffett Field, California.

30 July 1971; revised 1 October 1971 ■

Raman Scattering from Flames

Abstract. *Laser Raman scattering data for nitrogen, oxygen, and water vapor have been obtained from hydrogen-air and hydrogen-oxygen flames. The resulting ground-state and upper-state vibrational bands exhibit strong asymmetrical broadening. Experimental spectral profiles have been fitted theoretically to give a new measurement technique for the determination of rotational and vibrational excitation temperatures.*

We report here observations of vibrational Raman scattering from flame gases. One motivation for these observations is that Raman scattering can provide spatially resolved measurements of the concentration and the vibrational and rotational excitation temperatures of flame constituents. This capability should prove to be of substantial use in the diagnostics of nonequilibrium as well as equilibrium phenomena.

The work presented here is focused upon the observation of temperature-dependent effects in the spectral distribution of the Stokes Q-branch vibrational scattering. These effects arise predominantly from the vibration-rotation interaction and from significant populations of excited vibrational levels. From these excited levels originate upper-state bands (*1*) which are usually shifted toward the blue region of the spectrum.

In Fig. 1 we show the types of fundamental vibrational Raman scattering events that may be observed in flames. Earlier Raman scattering experiments at elevated temperatures have dealt with laser heating of a vapor (*2*), with studies of species in ovens at temperatures up to 1000°C (*3*), and with a low-pressure electric discharge (*4*). We have been unable to find any earlier publications concerning Raman scattering in flames or in any systems at temperatures in excess of 1000°C.

Our initial observations were confined to Stokes bands arising from 4880-Å incident radiation from an argon ion laser (Coherent Radiation model 52B) operated for most data at 1.5 watts. The scattered light was analyzed by a double monochromator (Spex 1400-II) with 5000-Å blazed gratings. The detector was a cooled photomultiplier (RCA C31000E Quantacon) operated in the pulse-counting mode with dark current levels of about 18 counts per second for this work.

The overall experimental arrangement was designed to have the laser beam traveling along the direction of the entrance slits (that is, vertically) and focused at a position about 0.3 m from the entrance slits. The Raman-scattered radiation was collected by a multielement lens with a focal length of 75 mm. The width of the laser beam in the scattering zone was about 100 μm, and the height from which the scattered radiation was accepted (as determined by the 1-cm slit height and the image magnification factor of 2) was about 5 mm. The monochromator entrance and exit slits were set to 300 μm, for which the spectral slit width was measured to be in very close agreement with the value calculated from the instrument dispersion curve. The (Rayleigh and Mie scattering) image of the laser beam at the entrance slits (as viewed by a periscope attachment behind the slits) showed no change when the flame was ignited.

The flames studied were produced on a water-cooled porous plug burner (diameter, 2.5 cm) (*5*) operated horizontally and burned into another water-cooled porous plug (of larger diameter) placed about 1.5 cm away which was, in turn, connected to a rough vacuum line. In this fashion, a stable horizontal flame at atmospheric pressure was produced which possessed the advantage of offering a scattering test zone of uniform conditions (that is, at a constant distance from the flat flame front) for a laser beam passing in the vertical direction. Scattering data for H_2O and O_2 were obtained from lean H_2-O_2 flames, whereas data for N_2 was obtained from a lean H_2-air flame. Because of the low luminosity of these flames in the spectral regions of interest, no increase in background was observed when the flames were ignited. Precise flow data were not taken, nor were accurate independent temperature measurements made, since the major goal of this portion of our flame Raman scattering investigation was the exploration of general temperature-sensitive features of scattered bands. The temperatures actually determined from the scattering data are reasonable values for the flames used.

Although vibrational temperatures have been determined from the Stokes/anti-Stokes ratios of vibrational scattering (*2*, *6*), the same information is accessible from the Stokes scattering alone. Our initial attention to the latter is due in part to the greater sensitivity of our spectrometer and detector to the Stokes scattering. However, there is also a potential advantage to this approach which arises from the fact that temperature measurements from Stokes (or anti-Stokes) scattering alone involve a much smaller spectral range than with the corresponding measurements of Stokes/anti-Stokes ratios. Thus, in the former case it is easier to correct for the spectral variation of background, absorption, and spectrometer response.

The asymmetry of the vibrational bands is evident even at room temperature for the molecules considered here, and particularly so for H_2O. In Fig. 2B the H_2O vibrational ground-state band is shown for scattering from room temperature ambient H_2O. The greatly increased broadening toward the blue region of the spectrum under flame conditions is shown in Fig. 2A. The strong asymmetry of the N_2 and O_2 vibrational bands under flame conditions can be seen in Figs. 3 and 4. This "blue asymmetry" is explained by the fact that all the $\Delta J = 0$ rotational lines corresponding to the Q-branch do not overlap each other exactly. There is a progressive shift to shorter wavelengths caused by the vibration-rotation interaction term of the energy levels for a molecule. To discuss the spectral shape and position of each band, we consider the term value $G(v,J)$ for a real diatomic molecule (*7*), including contributions from harmonic and anharmonic oscillator terms, rigid and anharmonic rotor terms, and vibration-rotation interaction terms (*8*).

$$G(v,J) = E(v,J)/hc = \omega_e(v + \tfrac{1}{2}) - \omega_e x_e(v + \tfrac{1}{2})^2 + \omega_e y_e(v + \tfrac{1}{2})^3 + (B_e - \alpha_e/2)J(J+1) - (D_e + \beta_e/2)J^2(J+1)^2 - \alpha_e vJ(J+1) - \beta_e vJ^2(J+1)^2 + \dots \quad (1)$$

Here $E(v,J)$ is the energy of the level (v,J); h is Planck's constant; c is the

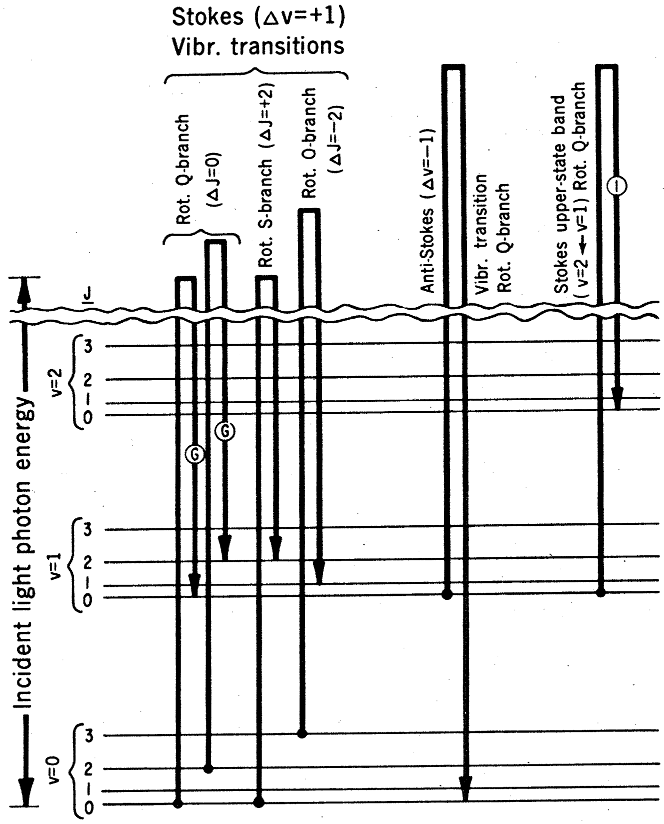

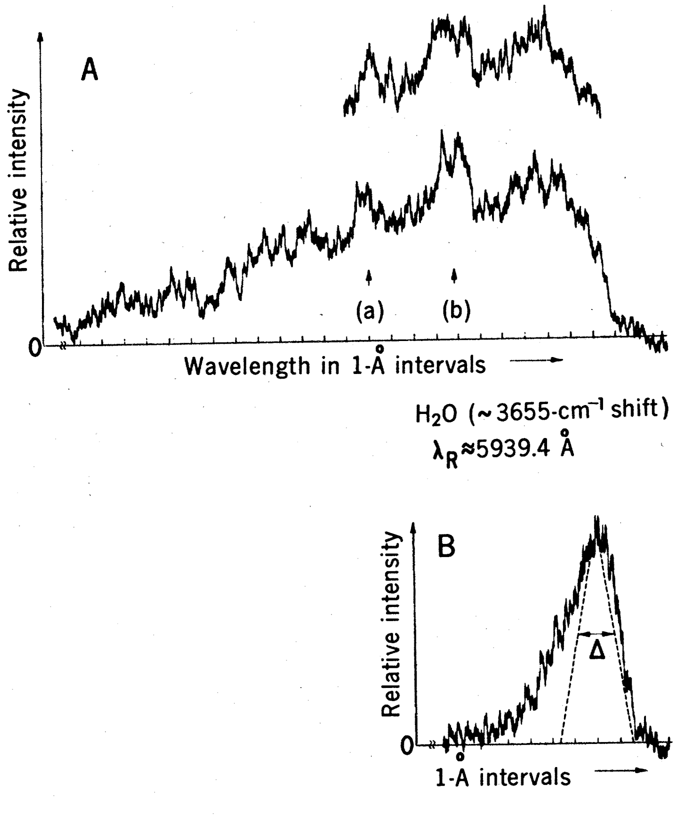

Fig. 1 (left). Schematic of some molecular transitions which contribute to fundamental vibrational Raman scattering ($\Delta v = \pm 1$). The Stokes upper-state band (circled numeral "one," at right) is associated with the molecular vibrational transition $v = 1$ to $v = 2$. For this transition the scattered photon energy is slightly greater than that for the ground state (that is, $v = 0$ to $v = 1$) Q-branch (circled letter "G") because of molecular vibrational anharmonicity. Thus, the upper-state band appears at a slightly shorter wavelength. Fig. 2 (right). (A) The H_2O Raman vibrational ground-state band for a lean H_2-O_2 flame. The partial segment above the full trace is a portion of another measurement shown to indicate the reproducibility of the gross features at positions (*a*) and (*b*). The latter is an upper-state band and is discussed at the end of this report. Although feature (*a*) approximately coincides with a weak Ar line at 5929 Å, experimental measurements failed to show sufficient scattering of this radiation to cause the observed signal. (B) The same H_2O Raman band taken in the laboratory atmosphere (295°K, 8 torr). The dashed curve is the spectrometer slit function. These curves correspond to 300-μm entrance and exit slits, for which the slit width Δ is 1.62 Å at this wavelength. The wavelength axes of these curves are indicated in a relative fashion only, since wavelength calibration lines were not included in the experiments and theoretical profiles have not yet been calculated. The wavelength $\lambda_R \approx 5934.5$ Å is slightly to the right of the peak of (*B*) (that is, at slightly longer wavelength). As an example of a case for which exact calculations are not complicated, the peak of the 295°K slit-convoluted profile for N_2 is at a wavelength about 0.3 Å less than the corresponding value of λ_R.

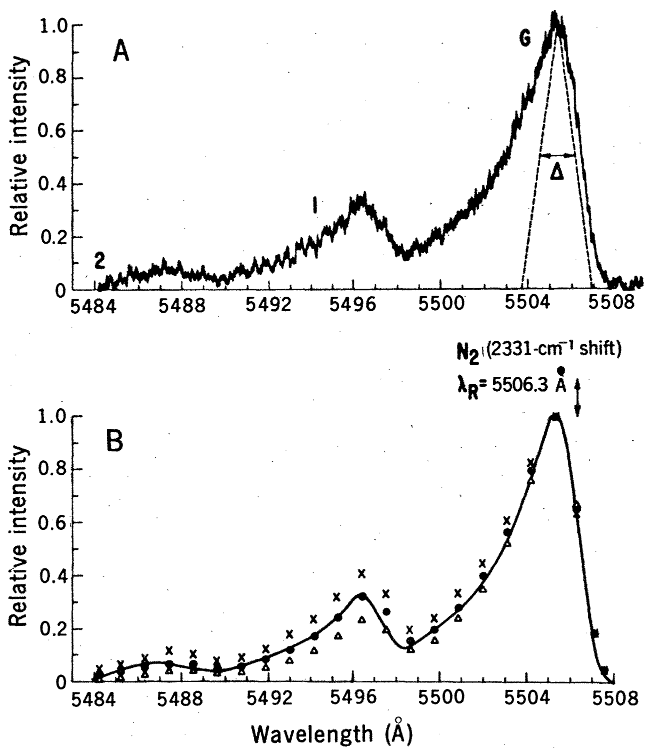

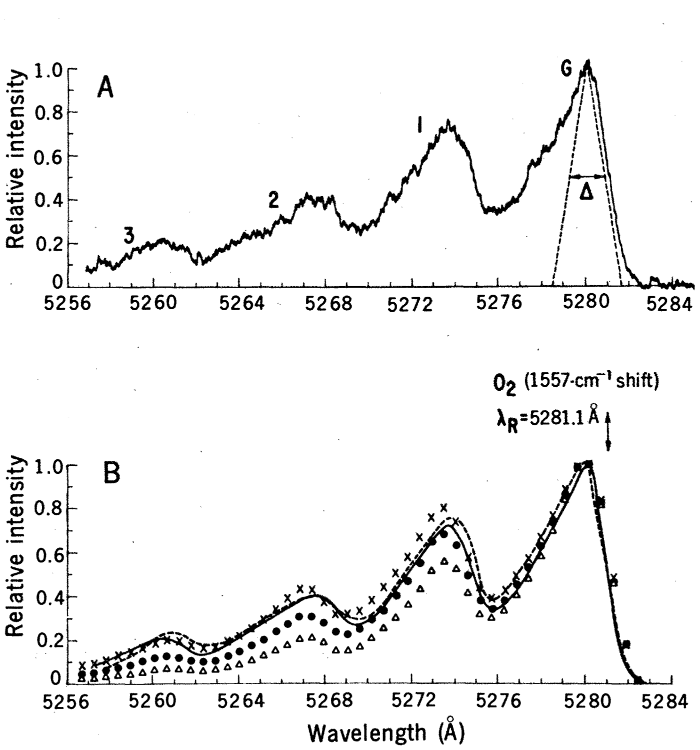

Fig. 3 (left). Raman scattering from N_2 in a lean H_2-air flame. (A) The experimental recording onto which has been superimposed the spectrometer slit function for the 300-μm entrance and exit slits used. The spectral slit width Δ is 1.63 Å. The labeling *G*, *1*, and *2* corresponds, respectively, to the ground-state Stokes vibrational Q-branch, the upper-state Q-branch ($v = 1$ to $v = 2$), and the upper-state Q-branch ($v = 2$ to $v = 3$). (B) The solid line is a tracing of the experimental curve (A), to facilitate comparison with the intensity calculated at discrete wavelengths from Eq. 3 at temperatures of 1400° (Δ), 1600° (●), and 1800°K (X). The fit of the theoretically calculated points for 1600°K with the experimental curve is quite close. Fig. 4 (right). (A) Raman scattering from O_2 in a lean H_2-O_2 flame. The general comments for Fig. 3 also apply here. However, in this case an additional upper-state band (labeled *3*) is seen. Furthermore, a tracing of a subsequent measurement under identical conditions is shown as the dashed curve in (B). These two curves give an estimate of the spread in the O_2 data, and are to be compared with the theoretically predicted shapes. An estimate of roughly 1700°K is obtained from these data.

speed of light; ω_e, $\omega_e x_e$, and $\omega_e y_e$ are vibrational constants such that $\omega_e y_e \ll \omega_e x_e \ll \omega_e$; B_e and D_e are, respectively, the rotational constants for rigid and nonrigid rotation in the equilibrium internuclear position; and α_e and β_e ($\alpha_e \ll B_e$ and $\beta_e \ll D_e$) represent vibration-rotation interactions.

The Raman shift for a fundamental vibrational band (that is, for $\Delta J = 0$ and $\Delta v = 1$) is, from Eq. 1,

$$\Delta G(v + 1, J \leftarrow v, J) = \omega_e - 2\omega_e x_e(v + 1) + \omega_e y_e(3v^2 + 6v + 13/4) - \alpha_e J(J + 1) - \beta_e J^2(J + 1)^2 + \ldots \quad (2)$$

where the vibration-rotation interaction, corresponding to the last two terms of Eq. 2, leads to the blue asymmetry for the bands. Here, β_e may be neglected, since $\beta_e \ll D_e \ll \alpha_e$.

The radiant flux *S* for a rotational line of the fundamental series ($v+1 \leftarrow v$) Stokes Raman-scattered Q-branch is given by (*9*, *10*)

$$S(v,J) \propto \frac{\eta\,(2J + 1)\,(v + 1)\,\omega_R{}^4 C_o}{Q_{rot}\,Q_{vib}} \exp\left[-\frac{hc}{kT}G(v,J)\right] \quad (3)$$

where *k* is Boltzmann's constant and ω_R is the wave number of the Raman fundamental line (*11*):

$$\omega_R = \omega_o - \Delta G(v + 1, J \leftarrow v, J)$$

for which ω_o is the wave number of the incoming (laser) radiation. Here, the depolarized contribution has been neglected, and the factors associated with the cross section which are not explicitly written out are denoted by c_o. The rotational (*12*) and vibrational partition functions Q_{rot} and Q_{vib} are, respectively,

$$Q_{rot} \approx kT/2hcB_e$$

$$Q_{vib} \approx [1 - \exp(-hc\omega_e/kT]^{-1}$$

and the factor η accounts for the effect of nuclear spin *I*. For N_2 ($I = 1$), the parity of the rotational levels is such that the symmetric levels correspond to even values of *J*, for which $\eta = 1$, whereas the antisymmetric levels correspond to odd values of *J*, for which $\eta = \frac{1}{2}$. For O_2 ($I = 0$), the symmetric levels correspond to odd values of *J*, for which $\eta = 1$, whereas the antisymmetric levels correspond to even values of *J*, for which $\eta = 0$ (that is, the lines corresponding to even values of *J* are missing).

It is evident from Eq. 3 that the shape of each particular band (that is, a given *v*) of the fundamental series will be dependent upon the rotational temperature, and that a proper fit to an experimental profile can then serve to determine this temperature. All of the bands of the fundamental series will have somewhat similar shapes. Here, for the purposes of illustration, we consider the ground-state band. The shape of this band (that is, the *S* versus ω profile) may be calculated from Eq. 3 which, for a fixed temperature, becomes

$$S(0,J) \propto (2J + 1)\,\omega_R{}^4 \times \exp\left[-hcB_e J(J + 1)/kT\right]$$

with

$$\omega_R \approx \omega_o - \omega_e + 2\omega_e x_e + \alpha_e J(J + 1)$$

where only those terms of quantitative significance which contribute to the relative band shape have been retained. The partition functions provide only a temperature-dependent scale factor for Eq. 3, and so are not of concern for profile fitting.

The experiments reported here corresponded with reasonable certainty to equilibrium populations for the vibrational and rotational energy levels. However, for situations in which equilibrium is not expected, the temperature factors appearing in the exponent of Eq. 3 can be denoted as values of T_{vib} or T_{rot} associated with particular energy levels, and the vibrational and rotational excitation temperatures corresponding to these degrees of freedom can therefore be determined. In general, the relative peak value or integrated intensity of each successive band indicates the vibrational temperature, whereas the shape (that is, blue asymmetry) of each band determines the rotational temperature. Thus, if nonequilibrium is suspected, separate fits to the shape of each band should be made. In this fashion, different vibrational and rotational excitation temperatures can be associated with each internal mode. This method should complement the well-studied OH emission and absorption techniques for the measurement of excitation temperatures, which have been applied to flames with success (*13*); conversely, this method might serve to determine anharmonic terms for species that have not yet been well studied (*14*).

For the case where equilibrium exists, relative values of $S(v,J)$ can be calculated as a function of wavelength over the entire spectral extent of the scattered bands for various temperatures and the results fitted to experimental curves. This has been done (*15*) for N_2 and O_2 in Figs. 3 and 4, with the result that the N_2 data closely fit 1600°K and the O_2 data roughly fit 1700°K. These values are reasonable for the flames used. We believe that these results demonstrate the utility of this Raman scattering method for the determination of flame temperatures, as well as for temperatures in a variety of other experimental and practical areas.

For H_2O, the analytical results are considerably more complicated since the calculations involve asymmetric top energy levels (*16*). However, if we consider only the purely vibrational contributions to the energy levels for an anharmonic nonlinear triatomic molecule (*17*), we can investigate in a qualitative fashion the lowest possible upper-state bands, where we use the notation (v_1,v_2,v_3) to denote the vibrational quantum numbers for the three fundamental vibrational modes. The band corresponding to the transition $(1,1,0) \leftarrow (0,1,0)$ is the most likely to be observed, since it arises from the population of the lowest excited vibrational level ($v_2 = 1$, 0.20 ev above the ground state). The separation $\delta\lambda$ between this upper-state band and the ground-state band (for no rotation) is $-x_{12}$, where x_{12} is the coefficient of the $(v_1 + ½)(v_2 + ½)$ term in the energy level expression. For H_2O, x_{12} is $-20.0\ \mathrm{cm}^{-1}$ and $\delta\lambda$ corresponds to a blue shift of 7.05 Å for incident 4880-Å radiation. This shift closely coincides with the position of feature (*b*) in Fig. 2A (since λ_R is located slightly to the right of the peak of the Raman scattering curve in Fig. 2B). Thus, we have evidence of an appreciable population of the H_2O $v_2 = 1$ level for the flame studied. More importantly, this result demonstrates the potential ability of Raman scattering measurements for polyatomic molecules.

In this report we have concentrated on temperature measurements. However, there is also substantial interest in the use of Raman scattering as a constituency probe in flames and other systems. One important point concerning such measurements is illustrated by the foregoing results. For systems wherein significant vibrational and rotational excitation occurs, temperature-dependent calculations, such as the ones we have discussed, are necessary (in addition to the basic cross section) in order to relate the scattering intensity over any specified bandwidth to the concentration of a particular constituent. Otherwise, significant errors in concentration analyses may be made, particularly in view of the fact that the total Q-branch scattering increases with vibrational excitation because of the factor $v + 1$ in the upper-state band scattering.

M. Lapp
L. M. Goldman
C. M. Penney

General Electric Company
Corporate Research and Development,
Schenectady, New York 12301

References and Notes

1. In other literature on Raman scattering and in infrared work these bands are often called hot bands, in reference to their appearance under thermally excited conditions. However, this phrase can be misleading, since upper-state bands can appear at low temperatures for species with low-lying vibrational energy levels. For example, Holzer *et al.* (*2*) have shown the importance of upper-state bands in Br_2 at room temperature. We have adopted the phrase "upper-state band" from R. M. Goody [*Atmospheric Radiation*, vol. 1, *Theoretical Basis* (Oxford Univ. Press, London, 1964), p. 81]. One further point of possible confusion lies in the conventional usage of vibrational "line" for the ground-state fundamental band. This terminology refers to the usually narrow Q-branches observed at room temperature, and so is not used here.
2. W. Holzer, W. F. Murphy, H. J. Bernstein, *J. Chem. Phys.* **52**, 399 (1970).
3. See, for a review, I. R. Beattie and G. A. Ozin, *Spex Speaker* **14**, No. 4 (Dec. 1969) (published by Spex Industries, Inc., Metuchen, N.J.).
4. J. J. Barrett and A. Weber, *J. Opt. Soc. Amer.* **60**, 70 (1970); L. Y. Nelson, A. W. Saunders, Jr., A. B. Harvey, G. O. Neeley, *J. Chem. Phys.*, in press.
5. See, for example, W. E. Kaskan, in *Sixth Symposium (International) on Combustion* (Reinhold, New York, 1957), pp. 134–143.
6. G. F. Widhopf and S. Lederman, *Amer. Inst. Aeronaut. Astronaut. J.* **9**, 309 (1971).
7. The essential results appear for the case of a diatomic molecule and are in good agreement with experimental results. Calculations for polyatomic molecules are necessarily more complicated.
8. G. Herzberg, *Molecular Spectra and Molecular Structure*, vol. 1, *Spectra of Diatomic Molecules* (Van Nostrand, Princeton, N.J., ed. 2, 1950), chap. 3. The spectroscopic constants subsequently used for N_2 and O_2 were taken from table 39.
9. ———, *ibid.*, chap. 3, sections 2(e) and 2(f); L. A. Woodward, in *Raman Spectroscopy*, H. A. Szymanski, Ed. (Plenum, New York, 1967), p. 35.
10. J. B. Tatum, *Astrophys. J. Suppl. Ser.* **14** (No. 124), 21 (1967).
11. In this development, the wave number ω_R is a function of both J and v. In Figs. 2, 3, and 4, the wavelength λ_R is not simply the reciprocal of ω_R but is defined as the wavelength corresponding to $J = 0$ for the ground-state vibrational band.
12. The rotational partition function given here is evaluated for a Σ state of a homonuclear molecule, which is the ground state for both N_2 and O_2. It includes the effect of nuclear spin [see (*10*)].
13. See, for example, S. S. Penner, *Quantitative Molecular Spectroscopy and Gas Emissivities* (Addison-Wesley, Reading, Mass., 1959), chap. 17; J. Anketell and R. C. M. Learner, *Proc. Roy. Soc. Ser. A Math. Phys. Sci.* **301**, 355 (1967), and references cited therein.
14. R. Gaufres and S. Sportouch, *C. R. Hebd. Seances Acad. Sci. Paris* **272**, 995 (1971).
15. The calculated relative intensity data in Figs. 3 and 4 were obtained from the convolution of $S(v,J)$ values from Eq. 3 with the experimentally determined monochromator slit function, which indicates the relative response of the monochromator to the wave number ω' when it is set at ω. These calculations were carried out through use of a computer. The slit function was found to be closely approximated by an isosceles triangle with only a very slight truncation. It is shown in Figs. 2A, 3A, and 4A normalized to the peaks of the ground-state bands. The spectral slit width Δ is the full width at half maximum. The inclusion of η in Eq. 3 is not really necessary here because Δ is sufficiently large to always include many rotational lines simultaneously. For example, 16 N_2 rotational lines are within the spectral range 2Δ (the base of the slit function profile) of the long-wavelength edge of the ground-state band. We have neglected the O-branch ($\Delta J = -2$) Raman lines from this work although they are in the spectral range of interest, since they do not contribute any significant intensity for the cases investigated here. Their omission would, however, make the intensities of high upper-state bands less certain.
16. G. Herzberg, *Molecular Spectra and Molecular Structure*, vol. 2, *Infrared and Raman Spectra of Polyatomic Molecules* (Van Nostrand, Princeton, N.J., 1945), chap. I, section 4, and chap. IV, section 4.
17. ———, *ibid.*, p. 205.

18. We are grateful to G. E. Moore for his help in the combustion aspects of these experiments.

17 September 1971; revised 3 November 1971